



Analysis of Empirical Probability of Detection Data for Dissimilar Metal Welds

July 2019

Ryan M. Meyer
Aimee E. Holmes



Prepared for the U.S. Nuclear Regulatory Commission
under a Related Services Agreement with the U.S. Department of Energy
CONTRACT DE-AC05-76RL01830

U.S. DEPARTMENT OF
ENERGY

DISCLAIMER

This report was prepared as an account of work sponsored by an agency of the United States Government. Neither the United States Government nor any agency thereof, nor Battelle Memorial Institute, nor any of their employees, makes **any warranty, express or implied, or assumes any legal liability or responsibility for the accuracy, completeness, or usefulness of any information, apparatus, product, or process disclosed, or represents that its use would not infringe privately owned rights.** Reference herein to any specific commercial product, process, or service by trade name, trademark, manufacturer, or otherwise does not necessarily constitute or imply its endorsement, recommendation, or favoring by the United States Government or any agency thereof, or Battelle Memorial Institute. The views and opinions of authors expressed herein do not necessarily state or reflect those of the United States Government or any agency thereof.

PACIFIC NORTHWEST NATIONAL LABORATORY
operated by
BATTELLE
for the
UNITED STATES DEPARTMENT OF ENERGY
under Contract DE-AC05-76RL01830

Printed in the United States of America

Available to DOE and DOE contractors from the
Office of Scientific and Technical Information,
P.O. Box 62, Oak Ridge, TN 37831-0062;
ph: (865) 576-8401
fax: (865) 576-5728
email: reports@adonis.osti.gov

Available to the public from the National Technical Information Service
5301 Shawnee Rd., Alexandria, VA 22312
ph: (800) 553-NTIS (6847)
email: orders@ntis.gov <<https://www.ntis.gov/about>>
Online ordering: <http://www.ntis.gov>

Analysis of Empirical Probability of Detection Data for Dissimilar Metal Welds

Ryan M. Meyer
Aimee E. Holmes

July 2019

Prepared for
the U.S. Nuclear Regulatory Commission
under a Related Services Agreement
with the U.S. Department of Energy
Contract DE-AC05-76RL01830

Pacific Northwest National Laboratory
Richland, Washington 99352

Summary

The U.S. Nuclear Regulatory Commission's (NRC) Standard Review Plan (SRP) 3.6.3 describes leak-before-break (LBB) assessment procedures that can be used to assess compliance with the 10 CFR 50 Appendix A, General Design Criteria (GDC)-4 requirement that primary system pressure piping exhibit an extremely low probability of rupture. SRP 3.6.3 does not allow for assessment of piping systems with active degradation mechanisms, such as primary water stress corrosion cracking (PWSCC), which is currently occurring in systems that have been granted LBB approvals. To address those piping systems approved for LBB that are experiencing PWSCC, the NRC Office of Nuclear Regulatory Research (RES) working cooperatively with the Electric Power Research Institute (EPRI) conducted a multi-year project to develop a probabilistic fracture mechanics code called eXtremely Low Probability of Rupture (xLPR) that can be used to assess compliance with the regulations.

xLPR is a probabilistic computational tool capable of evaluating degradation in reactor coolant piping welds leading to rupture with extremely low probabilities of occurrence. This tool models the effects of active degradation mechanisms and the inspection and mitigation activities that are being undertaken to manage PWSCC degradation. Crack initiation and growth due to fatigue and primary water stress corrosion, along with mitigation methods (mechanical mitigation as well as chemical mitigation) and the effects of in-service inspection (ISI) and leak detection can be analyzed using this tool.

One of the modules in xLPR is the ISI module, which models the probability of detection (POD) and sizing performance of nondestructive examination (NDE) performed during ISI to account for and predict the influence of periodic inspections on the probability of component leakage and rupture. The ISI module calculates the POD and the probability of repair for each crack.

The accuracy of the ISI module in xLPR is dependent on the quality of the estimates of detection and sizing performance that are input to the module. The most extensive source of empirical data from which estimates of detection and sizing performance can be obtained come from the data accumulated as part of the industry's Performance Demonstration Initiative (PDI). In addition to the PDI data, empirical detection and sizing performance data has been generated for dissimilar metal weld (DMW) components as part of the NRC-supported round robin studies—Program for Inspection of Nickel Alloy Components (PINC) and Program to Assess the Reliability of Emerging Nondestructive Techniques (PARENT). The purpose of this report is to examine the detection performance data that has been generated by these efforts in the context of using the data as input to the xLPR ISI module. A significant function of this report is to concisely summarize POD models for DMW components that have been generated from empirical data. In xLPR, POD models are defined by inputting beta parameters, their standard deviations, and their covariance for logistic function expressions. For convenience, a table of beta parameters, their standard deviations, and their covariances for POD models for small-bore DMW (SBDMW) and large-bore DMW (LBDMW) components obtained from PINC, PARENT, and PDI data analysis is included in Table S.1.

Detection performance data from the empirical studies are reviewed and comparatively analyzed as a function of flaw depth for DMW components. Comparisons of POD results are provided for both axial and circumferential flaws in SBDMW and LBDMW components with consideration also given to surface access (inner diameter [ID] or outer diameter [OD]). In general, significant variability between results is observed, especially for smaller flaw sizes. The PDI results provide the most conservative POD estimates for larger flaw sizes except for axial flaws in SBDMW components. Conversely, PINC or PARENT results provide more conservative results for smaller flaw sizes.

Table S.1. Summary of POD Model “Beta” Parameters for the Models Summarized in Sections 4.0 and 5.0

Category	Flaw Orientation	Data Source	β_1	β_2	σ_{β_1}	σ_{β_2}	$\rho_{\beta_1\beta_2}$	Min. Flaw Depth, x	Max. Flaw Depth, x	
SBDMW (OD Access)	Circumferential	PDI – Category A (MRP-262 Rev. 3; Table 6-8)	2.71	0.31	0.21	0.45	-0.86	0.10 ^(a)	1.00 ^(a)	
		PINC		-1.18	6.9	0.14	1.0	-0.49	0.10	0.83
		PARENT		-2.71	13.7	0.18	1.5	-0.48	0.03	0.72
SBDMW (OD Access)	Axial	PDI – Category A (MRP-262 Rev. 3; Table 6-5)	0.12	5.24	0.27	1.02	-0.91	0.10 ^(a)	1.00 ^(a)	
		PINC		-1.34	4.99	0.15	0.77	-0.46	0.11	0.71
		PARENT		-3.56	15.1	0.23	2.3	-0.43	0.11	0.74
SBDMW (ID Access)	Circumferential	PINC	-1.6	35.1	0.28	8.9	-0.23	0.10	0.83	
SBDMW (ID Access)	Axial	PINC	-1.57	25.4	0.27	8.0	-0.24	0.11	0.71	
LBDMW (ID Access)	Circumferential	PDI – Category B1 (MRP-262 Rev. 3; Table 6-14)	3.24	1.06	0.55	1.32	-0.87	0.10 ^(a)	1.00 ^(a)	
		PARENT		-3.31	56	0.29	13	-0.33	0.01	0.36
LBDMW (ID Access)	Axial	PDI – Category B1 (MRP-262 Rev. 3; Table 6-11)	2.50	0.82	0.51	1.40	-0.87	0.10 ^(a)	1.00 ^(a)	
		PARENT		-3.14	17.4	0.35	3.9	-0.40	0.01	0.36
LBDMW (OD Access)	Circumferential	PARENT	-2.91	14.3	0.22	2.7	-0.37	0.01	0.36	
LBDMW (OD Access)	Axial	PARENT	-3.08	10.5	0.22	1.6	-0.46	0.01	0.36	
LBDMW (OD Access)	Circumferential	PDI – Category B2 (MRP-262 Rev. 3; Table G-4)	5.41	0.86	3.64	6.02	-0.92	0.10 ^(a)	1.00 ^(a)	

(a) Minimum and maximum flaw sizes indicated for PDI datasets are based on the flaw size distribution requirements in Supplement 10 of Appendix VIII of Section XI of the American Society of Mechanical Engineers Boiler & Pressure Vessel Code and may not reflect the actual minimum and maximum flaw sizes in the PDI datasets.

Overall, the following general observations can be made from the summarized POD models for PINC, PARENT, and industry PDI data:

- Significant variability exists between the POD models obtained from analysis of data from PINC, PARENT, and industry PDI data.
- Variability in POD models obtained from each data set is greater for “small” flaw size regimes than “large” flaw size regimes.
- Some of the observed variability in POD models can be attributed to inconsistencies in the way data from each study is analyzed.

- A preliminary comparison of the POD models with some reported industry events was unable to yield firm conclusions regarding how well models represent actual field POD.

Based on the observations above, the following suggestions for future work are provided:

- Perform sensitivity analyses to better understand the importance of the observed variability in POD models.
- Develop standard guidance for analyzing data from PINC, PARENT, and PDI.
- Perform a systematic review of field events, and then compare field events with the POD models obtained from PINC, PARENT, and PDI data.

Acknowledgments

The authors express appreciation to Bruce Lin and Carol Nove of the U.S. Nuclear Regulatory Commission (NRC) for providing input and guidance on this effort and for their roles as alternative and primary Contracting Officer Representatives overseeing this effort. The authors would also like to thank Ms. Kay Hass for typing and editing this document.

Acronyms and Abbreviations

DMW	dissimilar metal weld
EPRI	Electric Power Research Institute
FCP	false call probability
GDC	General Design Criteria
ID	inner diameter
ISI	in-service inspection
LBB	leak-before-break
LBDMW	large-bore dissimilar metal weld
MLE	maximum likelihood estimation
NDE	nondestructive examination
NRC	U.S. Nuclear Regulatory Commission
OD	outer diameter
PARENT	Program to Assess the Reliability of Emerging Nondestructive Techniques
PAUT	phased array ultrasonic testing
PD	potential drop technique
PDI	Performance Demonstration Initiative
PINC	Program for Inspection of Nickel Alloy Components
POD	probability of detection
PWSCC	primary water stress corrosion cracking
RES	Office of Nuclear Regulatory Research
RPV	reactor pressure vessel
SBDMW	small-bore dissimilar metal weld
SRP	Standard Review Plan
TOFD	time-of-flight diffraction
TW	through wall
UT	ultrasonic testing
WOL	weld overlay
WSC	weld solidification crack
xLPR	eXtremely Low Probability of Rupture

Definitions

Dissimilar metal weld (DMW)	weldments joining components made of different alloys – In this context, it refers primarily to nozzle welds.
False call probability (FCP)	the likelihood that an inspection will provide an indication of detection when no structural defect is present
Performance Demonstration Initiative (PDI)	the program by which the U.S. nuclear industry implements requirements described by Appendix VIII of Section XI of the American Society of Mechanical Engineers Boiler & Pressure Vessel Code for the qualification of ultrasonic procedures, personnel and equipment
Primary water stress corrosion cracking (PWSCC)	the intergranular or interdendritic cracking of nickel-base alloys that occurs in service and originates from the surfaces of a component that are wetted by the primary water of a pressurized water reactor (PWR)
Probability of detection (POD)	the de facto metric used in quantifying the performance of an inspection for detecting structural defects (usually cracks) – The term reflects the stochastic nature of detection and has a value often expressed as a percentage (range from 0% to 100%) or fraction (range from 0 to 1). It is usually represented as a function of flaw size in this context.
Probability of leakage and rupture	a term used to quantitatively represent the likelihood of a reactor coolant piping experiencing a stable through-wall crack exhibiting detectable leakage or catastrophic failure (rupture)
Probability of repair	the likelihood that the outcome of detection of a crack in a component results in the mending of the component such that function is restored to an acceptable level for continued usage
Program to Assess the Reliability of Emerging NDE Techniques (PARENT)	an international cooperative research program that followed on to PINC – The purpose of PARENT was to address follow-on questions from PINC.
Program for the Inspection of Nickel-Alloy Components (PINC)	an international cooperative research program – The purpose of PINC was to assess the capabilities of current and emerging NDE techniques to detect and size flaws associated with PWSCC in nuclear reactors.
Round-robin test (RRT)	a test performed independently several times (usually at multiple testing facilities)
eXtremely Low Probability of Rupture (xLPR)	a modular-based probabilistic computational tool capable of determining probability of leakage and rupture for reactor coolant piping.

Contents

Summary	iii
Acknowledgments.....	vi
Acronyms and Abbreviations	vii
Definitions.....	viii
1.0 Introduction	1.1
1.1 Objectives.....	1.1
1.2 Organization of Report.....	1.2
2.0 Background.....	2.1
2.1 Logistic Regression Model of Probability of Detection.....	2.1
2.2 Analysis of Probability of Detection in MRP-262	2.3
2.3 False Call Probability	2.3
2.4 Uncertainty in Probability of Detection	2.4
2.5 MRP-262 Rev. 3 Models Referred to in this Report.....	2.4
2.6 Defining POD Models in xLPR	2.5
3.0 Scope of Nondestructive Examination Procedures and Techniques	3.1
4.0 Probability of Detection for Small Bore Dissimilar Metal Weld Components	4.1
4.1 Probability of Detection for Circumferential Flaws in Small Bore Dissimilar Metal Weld Components	4.1
4.2 Probability of Detection for Axial Flaws in Small Bore Dissimilar Metal Weld Components.....	4.3
4.3 Probability of Detection for Inner Diameter Access to Small Bore Dissimilar Metal Weld Components	4.5
5.0 Probability of Detection for Large Bore Dissimilar Metal Weld Components	5.1
5.1 Probability of Detection for Circumferential Flaws in Large Bore Dissimilar Metal Weld Components	5.1
5.2 Probability of Detection for Axial Flaws in Large Bore Dissimilar Metal Weld Components.....	5.3
5.3 Probability of Detection for Outer Diameter Access to Large Bore Dissimilar Metal Weld Components	5.5
5.4 Probability of Detection for Outer Diameter Access of PDI Category B2 (Steam Generator Nozzle) Components	5.7
6.0 Discussion of Empirical Probability of Detection Analysis Results	6.1
6.1 Small Bore Dissimilar Metal Weld Probability of Detection Results.....	6.1
6.2 Large Bore Dissimilar Metal Weld Probability of Detection Results.....	6.1
6.3 Contributions to Discrepancies in Results.....	6.2
6.4 Relevance of Results to the Field.....	6.3
6.5 Recommendations	6.4
7.0 Summary and Conclusions	7.1
8.0 References	8.1

Figures

Figure 2.1. Illustration of a POD Curve.....	2.2
Figure 4.1. Plots of POD as a Function of Flaw Depth (fraction of TW, x) for Circumferentially Oriented Flaws in SBDMW Test Blocks in PINC, PARENT, and PDI Efforts (OD Access)	4.2
Figure 4.2. Plots of POD as a Function of Flaw Depth (fraction of TW, x) for Axially Oriented Flaws in SBDMW Test Blocks in PINC, PARENT, and PDI Efforts (OD Access).....	4.4
Figure 4.3. POD as a Function of Flaw Depth (fraction of TW, x) for Circumferentially Oriented Flaws in SBDMW Test Blocks in PINC (ID Access)	4.6
Figure 4.4. POD as a Function of Flaw Depth (fraction of TW, x) for Axially Oriented Flaws in SBDMW Test Blocks in PINC (ID Access).....	4.6
Figure 5.1. Plots of POD as a Function of Flaw Depth (fraction of TW, x) for Circumferentially Oriented Flaws in LBDMW Test Blocks in PARENT and PDI Efforts (ID Access)	5.2
Figure 5.2. Plots of POD as a Function of Flaw Depth (fraction of TW, x) for Axially Oriented Flaws in LBDMW Test Blocks in PARENT and PDI Efforts (ID Access)	5.4
Figure 5.3. POD as a Function of Flaw Depth (fraction of TW, x) for Circumferentially Oriented Flaws in LBDMW Test Blocks in PARENT (OD Access).....	5.6
Figure 5.4. POD as a Function of Flaw Depth (fraction of TW, x) for Axially Oriented Flaws in LBDMW Test Blocks in PARENT (OD Access)	5.6
Figure 5.5. POD as a Function of Flaw Depth (fraction of TW, x) for Circumferentially Oriented Flaws in PDI Category B2 Components (EPRI 2017)	5.8

Tables

Table 2.1. Tabulated Summary of General Test Block Dimensions for Data Collected as Part of PDI, PINC, and PARENT	2.1
Table 2.2. Cross Reference to MRP-262 Rev. 3 for Curve Parameters Used in Sections 4 and 5.....	2.5
Table 3.1. Summary of PINC Procedures Used to Support Analysis of PINC Data for SBDMW Test Blocks by OD Access in Sections 4.1 and 4.2.....	3.1
Table 3.2. Summary of PINC Procedures Used to Support Analysis of PINC Data for SBDMW Test Blocks by ID Access in Section 4.3	3.2
Table 3.3. Summary of PARENT Procedures Used to Support Analysis of POD for SBDMW Test Blocks by OD Access in Sections 4.1 and 4.2.....	3.2
Table 3.4. Summary of PARENT Procedures Used to Support Analysis of POD for LBDMW Test Blocks by ID Access in Sections 5.1 and 5.2	3.2
Table 3.5. Summary of PARENT Procedures Used to Support Analysis of POD for LBDMW Test Blocks by OD Access in Section 5.3.....	3.3
Table 4.1. Tabulation of POD at Discrete Flaw Depth Sizes (fraction of TW, x) for Circumferentially Oriented Flaws in SBDMW Test Blocks in PINC, PARENT, and PDI Efforts	4.2

Table 4.2. Summary of the “Beta” Parameters Defining the Logistic Functions and Uncertainties for POD Curves Generated in Figure 4.1 for Circumferentially Oriented Flaws in SBDMW Test Blocks for PINC, PARENT, and PDI Efforts.....	4.3
Table 4.3. Tabulation of POD at Discrete Flaw Depth Sizes (fraction of TW, x) for Axially Oriented Flaws in SBDMW Test Blocks in PINC, PARENT, and PDI Efforts	4.4
Table 4.4. Summary of the “Beta” Parameters Defining the Logistic Functions and Uncertainties for POD Curves Generated in Figure 4.2 for Axially Oriented Flaws in SBDMW Test Blocks for PINC, PARENT, and PDI Efforts	4.5
Table 4.5. Tabulation of POD at Discrete Flaw Depth Sizes (fraction of TW, x) for POD Curves Generated in Figure 4.3 (circumferential flaws) and Figure 4.4 (axial flaws) for SBDMW Test Blocks and for ID Access for PINC	4.7
Table 4.6. Summary of the “Beta” Parameters Defining the Logistic Functions and Uncertainties for POD Curves Generated in Figure 4.3 (circumferential flaws) and Figure 4.4 (axial flaws) for SBDMW Test Blocks and for ID Access for PINC	4.7
Table 5.1. Tabulation of POD at Discrete Flaw Depth Sizes (fraction of TW, x) for Circumferentially Oriented Flaws in LBDMW Test Blocks in PARENT and PDI Efforts (ID Access).....	5.2
Table 5.2. Summary of the “Beta” Parameters Defining the Logistic Functions and Uncertainties for POD Curves Generated in Figure 5.1 for Circumferentially Oriented Flaws in LBDMW Test Blocks for PARENT and PDI Efforts (ID Access).....	5.3
Table 5.3. Tabulation of POD at Discrete Flaw Depth Sizes (fraction of TW, x) for Axially Oriented Flaws in LBDMW Test Blocks in PARENT and PDI Efforts (ID Access)	5.4
Table 5.4. Summary of the “Beta” Parameters Defining the Logistic Functions and Uncertainties for POD Curves Generated in Figure 5.2 for Axially Oriented Flaws in LBDMW Test Blocks for PARENT and PDI Efforts (ID Access)	5.5
Table 5.5. Tabulation of POD at Discrete Flaw Depth Sizes (fraction of TW, x) for POD Curves Generated in Figure 5.3 (circumferential flaws) and Figure 5.4 (axial flaws)	5.7
Table 5.6. Summary of the “Beta” Parameters Defining the Logistic Functions and Uncertainties for POD Curves Generated in Figure 5.3 (circumferential flaws) and Figure 5.4 (axial flaws)	5.7
Table 5.7. Summary of the “Beta” Parameters Defining the Logistic Functions and Uncertainties for POD Curves Generated in Figure 5.5.....	5.8
Table 6.1. Summary of Leakage Events from Appendix A and B of NUREG/CR-7187 (Sullivan and Anderson 2014)	6.4
Table 6.2. Summary of POD Model “Beta” Parameters for the Models Summarized in Sections 4.0 and 5.0.....	6.5

1.0 Introduction

The U.S. Nuclear Regulatory Commission's (NRC) Standard Review Plan (SRP) 3.6.3 describes leak-before-break (LBB) assessment procedures that can be used to assess compliance with the 10 CFR 50 Appendix A, General Design Criteria (GDC)-4 requirement that primary system pressure piping exhibit an extremely low probability of rupture (NRC 2007). SRP 3.6.3 does not allow for assessment of piping systems with active degradation mechanisms, such as primary water stress corrosion cracking (PWSCC), which is currently occurring in systems that have been granted LBB approvals. To address those piping systems approved for LBB that are experiencing PWSCC, the NRC Office of Nuclear Regulatory Research (RES) working cooperatively with the Electric Power Research Institute (EPRI) conducted a multi-year project to develop a probabilistic fracture mechanics code called eXtremely Low Probability of Rupture (xLPR) that can be used to assess compliance with the regulations.

xLPR is a modular-based probabilistic computational tool capable of determining probability of leakage and rupture for reactor coolant piping. This tool incorporates a set of deterministic models that represent the full range of physical phenomena necessary to evaluate both fatigue and PWSCC degradation mechanisms from crack initiation through failure (Rudland et al. 2015).

One of the modules in xLPR is the in-service inspection (ISI) module which models the probability of detection (POD) and sizing performance of nondestructive examination (NDE) performed during ISI to account for and predict the influence of periodic inspections on the probability of component leakage and rupture. The ISI module calculates the POD and the probability of repair for each crack.

The accuracy of the ISI module in xLPR is dependent on the quality of the estimates of detection and sizing performance that are input to the module. The most extensive source of empirical data from which estimates of detection and sizing performance can be obtained come from the data accumulated as part of the industry's Performance Demonstration Initiative (PDI). A description of the analysis performed to develop detection and sizing performance estimates from the industry PDI database is provided in report MRP-262 Rev. 3 (EPRI 2017), which provides these estimates for several component types. In addition to the PDI data, empirical detection and sizing performance data has been generated for dissimilar metal weld (DMW) components as part of the NRC-supported round robin studies —Program for Inspection of Nickel Alloy Components (PINC; Cumblidge et al. 2010) and Program to Assess the Reliability of Emerging Nondestructive Techniques (PARENT; Meyer and Heasler 2017).

1.1 Objectives

The purpose of this report is to examine the detection performance data that has been generated by PINC, PARENT, and PDI in the context of using the data as input to the xLPR ISI module. More specifically, a significant objective of this report is to generate guidance for users of xLPR with respect to implementation of empirical performance data from PINC, PARENT, and PDI. To achieve the above objective, detection performance data from the empirical studies are reviewed and comparatively analyzed as a function of flaw depth for DMW components. A review of this data attempts to highlight consistencies and inconsistencies between the data sets.

1.2 Organization of Report

Section 2.0 of this report provides a summary of relevant background information including overviews of the PDI, PINC, and PARENT analyses and the POD models used for these studies and in xLPR.

Section 3.0 summarizes the NDE procedures and techniques for which the PINC and PARENT data reported in Sections 4.0 and 5.0 are based on. Sections 4.0 and 5.0 present POD data collected for SBDMWs and for LBDMWs, respectively, in PDI, PINC, and PARENT in a way to facilitate analysis of consistencies and inconsistencies in the results. Section 6.0 includes a discussion of this comparative analysis highlighting similarities and inconsistencies. Further discussion of the relevancy of results with field data is included. Section 7.0 includes a summary of conclusions from the analysis, and references cited in this report are provided in Section 8.0.

2.0 Background

Inspection data collected as part of PDI was analyzed to develop quantitative estimates of detection and sizing performance that could be input to the ISI module of xLPR. The purpose of the industry PDI is the qualification of ultrasonic procedures, personnel, and equipment in accordance with requirements described by Appendix VIII of Section XI of the American Society of Mechanical Engineers Boiler & Pressure Vessel Code. In the United States, Appendix VIII is implemented through a pass/fail screening test administered by PDI.

Initially, analysis of PDI inspection data focused on data collected from three categories of components as documented in the first revision of report MRP-262 (Ammirato 2009). These categories included pressurizer surge and hot-leg surge components (referred to as Category A), reactor pressure vessel (RPV) inlet and outlet nozzles (referred to as Category B1), and steam generator inlet and outlet nozzles (referred to as Category B2). Further, this initial analysis focused only on circumferentially oriented flaws as they are considered more significant with respect to causing possible component rupture. This analysis has been expanded and updated in Revision 3 of MRP-262 (EPRI 2017). Revision 3 incorporated results from analysis performed on axially oriented flaws and data collected from weld overlays (WOLs).

The NRC has sponsored multiple round robin studies to quantify the performance of NDE for reactor coolant pressure boundary piping components beginning in the early 1980s. The most recent studies conducted include PINC (Cumblidge et al. 2010) and PARENT (Meyer and Heasler 2017). The PINC study focused on SBDMW components. In PARENT, data was collected on both SBDMW components and LBDMWs. The SBDMWs are most consistent in size to the pressurizer surge and hot-leg surge components (referred to as Category A), examined as part of PDI based on component diameter and wall thickness while LBDMWs are most consistent with RPV inlet and outlet nozzles (referred to as Category B1) examined as part of PDI. A summary of general test block dimensions for the PDI, PINC, and PARENT data sets is provided in Table 2.1.

Table 2.1. Tabulated Summary of General Test Block Dimensions for Data Collected as Part of PDI, PINC, and PARENT

	PDI		PINC		PARENT	
	Pressurizer Surge (Category A)	Reactor Pressure Vessel (Category B1)	Steam Generator Nozzle (Category B2)	SBDMW	SBDMW	LBDMW
Outer Diameter (mm)	305–356	686–787	685–787	386–390	289 and 815	852–895
Wall Thickness (mm)	30–58	64–76	127–132	42–46	35 and 39.5	68–78
Access	OD	ID	OD	OD and ID	OD	OD and ID

ID = inner diameter; OD = outer diameter

2.1 Logistic Regression Model of Probability of Detection

The analysis of detection performance is based on quantification of POD. POD is a widely established metric for measuring the performance of NDE. Although POD can be represented as a function of multiple independent variables, it is often customary to represent POD as a function of flaw size, a , since the size of the flaw is especially relevant to structural integrity. In this case, POD is represented as a

monotonic curve versus a that can range from 0 for flaws below the detection threshold up to 1 for larger flaws. The ideal POD curve is a step function with perfect (POD = 1) detection of all flaws of $a > 0$ and no detection (POD = 0) of flaws of $a = 0$ (or $a \leq$ pre-defined minimum flaw size). However, because missed detections are more frequent for shallow flaws, most POD curves have an S-like shape as illustrated in Figure 2.1. POD curves with steeper slopes that plateau at lower flaw sizes indicate better detection capabilities than those that have shallow slopes or that fail to plateau.

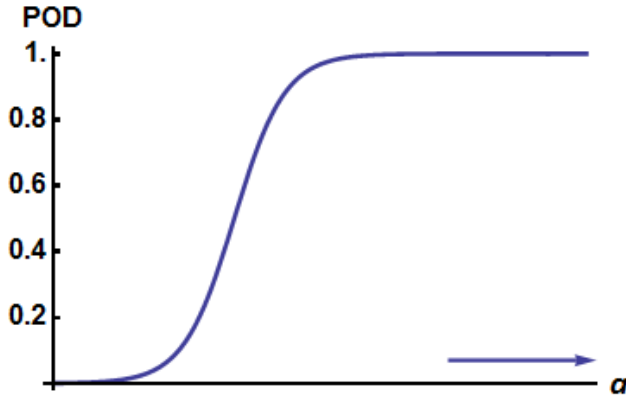


Figure 2.1. Illustration of a POD Curve

Mathematical models depicting the general relationship in Figure 2.1 are fit to empirically derived data to define an expression of POD that is continuous with respect to a . For empirical studies that generate binary NDE responses (hit/miss), the data can be fit with the logistic function (Berens 1989),

$$\text{POD}(a) = \frac{1}{1 + \exp(-\beta_1 - \beta_2 a)} = \frac{\exp(\beta_1 + \beta_2 a)}{1 + \exp(\beta_1 + \beta_2 a)} \quad (1)$$

This model includes two parameters, β_1 , and β_2 , to be determined from curve fitting with empirical data. In this equation, the parameters β_1 and β_2 are determined using maximum likelihood estimation (MLE) (Forsyth and Fahr 1998). This model was used to create POD curves from data collected in the PINC (Cumblidge et al. 2010) and the PARENT (Meyer and Heasler 2017) round robin studies, and is also the primary model used to fit data generated from the industry PDI program (EPRI 2017). Another way to write Eq. (1) is:

$$\log\left(\frac{\text{POD}(a)}{1 - \text{POD}(a)}\right) = \beta_1 + \beta_2 a \quad (2)$$

Here, a logit transformation is applied to the response ($\text{POD}(a)$) to change the problem into a linear regression problem on the logit-transformed response variable. In the analysis of data from PINC, PARENT, and the PDI program, the flaw size, a , is represented by the flaw depth x (normalized as a fraction of component through-wall [TW] thickness). When the flaw depth is normalized as a fraction of component thickness, the beta parameters in Eq. (1) relate a dimensionless flaw size to POD. In this case, the beta parameters are also dimensionless.

2.2 Analysis of Probability of Detection in MRP-262

In the analysis of PDI data, the model in Eq. (1) is applied over the range of flaw depths within the dataset, which is restricted to flaw depths greater than 0.1 TW for DMW test blocks (EPRI 2017). Therefore, no continuous expression of POD is derived for flaw depths less than 0.1 TW for DMW test blocks in PDI data. The ISI module in xLPR accepts piecewise representations of POD allowing for different model representations of POD over separate ranges of flaw depths. In this case, the ISI module of xLPR allows for a linear model of POD to be defined over the small flaw depth range while a model of the form of Eq. (1) is used to represent POD above the small flaw depth threshold, x_{small} . This is expressed by the function $POD_{PW}(x)$ as,

$$POD_{PW}(x) = \begin{cases} POD(x=0) + [POD(x_{small}) - POD(x=0)] * \left[\frac{x}{x_{small}} \right] & 0 < x < x_{small} \\ POD(x) & x_{small} \leq x < 1 \end{cases} \quad (3)$$

In this equation, the subscript, *PW*, denotes the piece-wise version of the POD model.

2.3 False Call Probability

In the PINC (Cumblidge et al. 2010) and the PARENT (Meyer and Heasler 2017) round-robin studies, the model represented by Eq. (1) is applied over a range of x that includes 0 TW using data collected from false calls to define POD at 0 TW. The formula for converting false call rate (# of false calls per length of examined material) to false call probability (FCP) is described in NUREG reports documenting the results from the PINC (Cumblidge et al. 2010) and PARENT studies (Meyer and Heasler 2017). Specifically, the method for calculating false call rate and FCP is described in Section 4.1.2 of Cumblidge et al. (2010). The same description is included in Section D.2 in Meyer and Heasler (2017). A false call is defined as a call that does not intersect with a flawed grading unit. These false calls were used to estimate a false call rate, λ_{fc} (false calls per meter),

$$\lambda_{fc} = \frac{\text{#False Calls}}{\text{Length of Unflawed Material Inspected}}. \quad (4)$$

In (4), the length of unflawed material inspected is determined by subtracting the length of flawed material inspected from the total length of material inspected.

Using the rate in Eq. (4) and the assumption that false calls are randomly (i.e., Poisson) distributed, the probability that a false call would intersect a blank grading unit of length L_{gu} can be calculated as follows.

$$FCP = \Pr(\text{Grading Unit Intersection}) = 1 - \exp(-\lambda_{fc}(L_{gu})). \quad (5)$$

The average length for the blank grading units should be approximately the same as the average length of flawed grading units so that the POD and FCP can be compared. The number of blank grading units are determined by rounding the total length of inspected unflawed material divided by the blank grading unit size, L_{gu} .

A distinction between the FCP and the value of POD at a (or x) = 0 is required as they are not necessarily the same. FCP is defined above, whereas POD(0) is the value of the fit curve representation of POD at a (or x) = 0. POD(0) will be influenced by the FCP and the detection performance data for a or $x > 0$.

If Eq. (1) is considered with $a = 0$, the implications of the β_1 value with respect to estimated POD(0) can be observed. In the limit of large negative values for β_1 (i.e., $\beta_1 \rightarrow -\infty$), POD(0) approaches 0, while in the limit of large positive values for β_1 (i.e., $\beta_1 \rightarrow \infty$), POD(0) approaches 1. For $\beta_1 = 0$, Eq. (1) results in $\text{POD}(0) = 0.5$.

In the analysis of PDI data documented in MRP-262 Rev. 3 (EPRI 2017), false call rate data is not included in the creation of POD curves.

2.4 Uncertainty in Probability of Detection

The uncertainties in model parameters, β_1 , and β_2 , are represented by a covariance matrix from which the standard deviations in the model parameters, σ_{β_1} and σ_{β_2} , and the covariance in the model parameters, $\rho_{\beta_1\beta_2}$, can be estimated. In practice, this uncertainty is often expressed in terms of 95% confidence intervals, which are included on plots of the calculated POD. A wide confidence interval indicates that performance was variable and that there is less confidence in the POD for a given flaw depth. This may be due to inconsistency in detections or to a small number of data points, or both.

2.5 MRP-262 Rev. 3 Models Referred to in this Report

Results are presented for multiple scenarios in MRP-262 Rev. 3 (EPRI 2017). Generally, results are presented based on analysis performed on the population of passed examinations and on the total population of passed and failed examinations. Further, outlier data are considered in MRP-262 Rev. 3 and the results of analysis are provided for both cases of inclusion and exclusion of outlier data. In Sections 4.0 and 5.0, the results from MRP-262 Rev. 3 that are presented are based on the population of passed examinations and for the case in which outlier data is included in the analysis (denoted as “All Data”). Specifically, the PDI-based POD curves presented in Sections 4.0 and 5.0 are based on the curve parameters cross referenced in Table 2.2.

Significant validation work was performed for the analysis of PDI data and this is documented in MRP-262 Rev. 3. The models derived from PDI data selected in this report are based on the similarity in test block dimensions and flaw orientations for models derived from data in PINC and PARENT regardless of the status of validation. Interested readers are encouraged to refer to MRP-262 Rev. 3 for a discussion of the validation methods and results of validation.

Table 2.2. Cross Reference to MRP-262 Rev. 3 for Curve Parameters Used in Sections 4 and 5

Component Category	Flaw Orientation	Source of PDI Results Presented in Sections 4 and 5
Category A (pressurizer surge line)	Circumferential	MRP-262 Rev. 3; Table D-3 All Data
Category A (pressurizer surge line)	Axial	MRP-262 Rev. 3; Table D-1 All Data
Category B1 (RPV nozzle)	Circumferential	MRP-262 Rev. 3; Table D-7 All Data
Category B1 (RPV nozzle)	Axial	MRP-262 Rev. 3; Table D-5 All Data
Category B2 (steam generator nozzle)	Circumferential	MRP-262 Rev. 3; Table G-6 All Data

2.6 Defining POD Models in xLPR

The development of POD models for xLPR is based primarily on the models described in MRP-262 Rev. 3 (EPRI 2017). That is, xLPR allows for defining a piecewise function for POD combining a logistic function expression for flaw sizes greater than the small flaw depth threshold, x_{small} , and alternative functional fits for the flaw size range from $x = 0$ to $x = x_{small}$. Logistic function expressions are defined in xLPR by inputting the beta parameters, β_1 , and β_2 , the standard deviations in the beta parameters, σ_{β_1} and σ_{β_2} , and the covariance in the beta parameters, $\rho_{\beta_1\beta_2}$.

3.0 Scope of Nondestructive Examination Procedures and Techniques

The results of the POD analysis presented in this report for PINC and PARENT studies are based on data collected from established NDE procedures and techniques that are implemented in the field by commercial vendors. An NDE procedure comprises of one or more NDE techniques as part of the attempt to detect and analyze flaws. In PARENT, procedures were distinguished with an identifier expressed as “Tech1.Tech2...TechN.TeamID” where Tech1 through TechN represent all the techniques that were used for a given procedure and Team ID refers to a numerical identifier used to distinguish participating teams. Possible techniques include conventional ultrasonic testing (UT), phased-array ultrasonic testing (PAUT), eddy current testing (ECT), and time-of-flight diffraction ultrasonic testing (TOFD). For example, Team 117 employed a procedure that included a UT technique and a TOFD technique; thus, its procedure name is UT.TOFD.117. Interested readers may refer to Section 3.0 of NUREG/CR-7235 (Meyer and Heasler 2017) for a description of these techniques and can refer to Appendices B and C of NUREG/CR-7235 for details of specific procedures that were implemented in PARENT blind testing. The descriptions of techniques in Section 3.0 of NUREG/CR-7235 is also applicable to PINC (Cumblidge et al. 2010).

Tables 3.1 and 3.2 include summaries of the procedures used in PINC that support the analysis of POD in this report. These tables are compiled by combining information from Tables 4.3 and 4.8 in NUREG/CR-7019 (Cumblidge et al. 2010). Table 3.1 includes a summary of the outer diameter (OD) access techniques applied to SBDMWs in PINC and Table 3.2 includes a summary of the inner diameter (ID) access techniques applied to SBDMWs in PINC. Some potential drop (PD) techniques were also applied for OD and ID access inspections of SBDMWs in the PINC study but were excluded for the purposes of this analysis. The PD techniques were not included because their technological maturity is relatively low, and they are not employed in the field. Tables 3.1 and 3.2 indicate if the teams and procedures were qualified. In this case, qualification criteria are based on the requirements established by the country of the participating teams.

Table 3.1. Summary of PINC Procedures Used to Support Analysis of PINC Data for SBDMW Test Blocks by OD Access in Sections 4.1 and 4.2

Team	Techniques	Qualified Team	Qualified Procedure	Data Collection	Procedure ID (PARENT Convention)
13	PAUT	X	X	Automated	PAUT.13
22	UT		X	Automated	UT.22
28	UT	X	X	Automated	UT.28
30	UT	X	X	Manual	UT.30
39	PAUT		X	Automated	PAUT.39
48	UT	X	X	Manual	UT.48
63	UT		X	Automated	UT.63
66	UT and PAUT	X		Manual+Encoded	UT.PAUT.66
72	PAUT	X	X	Automated	UT.72
82	UT and TOFD		X	Automated	UT.TOFD.82

UT = conventional UT, PAUT = phased array UT, TOFD = time-of-flight diffraction UT

Table 3.2. Summary of PINC Procedures Used to Support Analysis of PINC Data for SBDMW Test Blocks by ID Access in Section 4.3

Team	Techniques	Qualified Team	Qualified Procedure	Data Collection	Procedure ID (PARENT Convention)
38	ECT			Manual+Encoded	ECT.38
70	ECT	X		Manual+Encoded	ECT.70
96	ECT	X	X	Automated	ECT.96

ECT = eddy current testing

A summary of the procedures used in PARENT for examination of SBDMWs is included in Table 3.3. All the procedures incorporate UT, PAUT, TOFD, or some combination of these techniques. All the procedures were considered qualified at the time of testing except for UT.25, which was undergoing a process for qualification. Summaries of procedures used in PARENT for examination of LBDMWS by ID and OD access are included in Tables 3.4 and 3.5, respectively.

According to MRP-262 Rev. 3, the reported POD results are based on the analysis of ultrasonic inspection data, which includes data from manual and automated conventional UT and PAUT techniques. MRP-262 Rev. 3 also provides POD results for procedures that passed qualification and POD results incorporating data from both passed and failed procedures.

Table 3.3. Summary of PARENT Procedures Used to Support Analysis of POD for SBDMW Test Blocks by OD Access in Sections 4.1 and 4.2

Team	Techniques	Qualified Team	Qualified Procedure	Data Collection	Procedure ID
25	UT	X		Automated	UT.25
115	PAUT	X	X	Manual	PAUT.115
128	PAUT	X	X	Automated	PAUT.128
117	UT and TOFD	X	X	Automated	UT.TOFD.117
108	UT	X	X	Manual	UT.108
108	PAUT	X	X	Manual	PAUT.108.1
134	UT	X	X	Manual	UT.134.2
126	UT	X	X	Manual	UT.126
126	PAUT	X	X	Manual	PAUT.126.1

UT = conventional UT, PAUT = phased array UT, TOFD = time-of-flight diffraction UT

Table 3.4. Summary of PARENT Procedures Used to Support Analysis of POD for LBDMW Test Blocks by ID Access in Sections 5.1 and 5.2

Team	Techniques	Qualified Team	Qualified Procedure	Data Collection	Procedure ID
101	ECT, UT, and TOFD	X	X	Automated	UT.TOFD.ECT.101
144	ECT and UT	X	X	Automated	UT.ECT.144
113	UT and PAUT	X	X	Automated	UT.PAUT.113
135	ECT	X	X	Manual+Encoded	ECT.135

UT = conventional UT, TOFD = time-of-flight diffraction UT, ECT = eddy current testing, PAUT = phased array UT

Table 3.5. Summary of PARENT Procedures Used to Support Analysis of POD for LBDMW Test Blocks by OD Access in Section 5.3

Team	Techniques	Qualified Team	Qualified Procedure	Data Collection	Procedure ID
108	UT	X	X	Manual	UT.108
108	PAUT	X	X	Manual	PAUT.108.1
134	UT	X	X	Manual	UT.134.2
126	UT	X	X	Manual	UT.126
126	PAUT	X	X	Manual+Encoded	PAUT.126.1

UT = conventional UT, PAUT = phased array UT

4.0 Probability of Detection for Small Bore Dissimilar Metal Weld Components

This section presents the results of POD analysis for SBDMW components in PINC, PARENT, and PDI. For PDI, Category A (pressurizer surge line) components are comparable to SBDMW test blocks in PINC and PARENT based on the similarity in dimensions. The reader may refer to Table 2.1 for an overview of these test block dimensions. Results are presented as POD versus fraction of TW depth, x , for OD access of SBDMWs for circumferentially and axially oriented flaws in Sections 4.1 and 4.2, respectively. A similar presentation of results for PINC SBDMW test blocks for ID access is provided in Section 4.3.

4.1 Probability of Detection for Circumferential Flaws in Small Bore Dissimilar Metal Weld Components

POD curves derived as a function of flaw depth for circumferentially oriented flaws in SBDMW test blocks in PINC, PARENT, and PDI efforts are presented in Figure 4.1. A tabulation of POD values from these curves at discrete flaw depth sizes is provided in Table 4.1. The beta parameters defining the logistic functions of the POD curves in Figure 4.1, and their uncertainties, is provided in Table 4.2. Here, and in the rest of this report, the beta parameters and their uncertainties for POD models are provided for those readers who wish to recreate the models. The range of flaw sizes included in each study is also provided in Table 4.2 to help readers judge suitability of the models for an application. These results are obtained for OD access to SBDMWs.

For the circumferential flaw results in Figure 4.1, it is evident that the analysis of PDI data produces an almost flat POD curve for flaw sizes greater than and equal to 0.1 TW. As a result, the PDI analysis predicts much higher POD for small flaw sizes than PINC or PARENT and predicts a smaller POD for larger flaw sizes in comparison to PINC or PARENT.

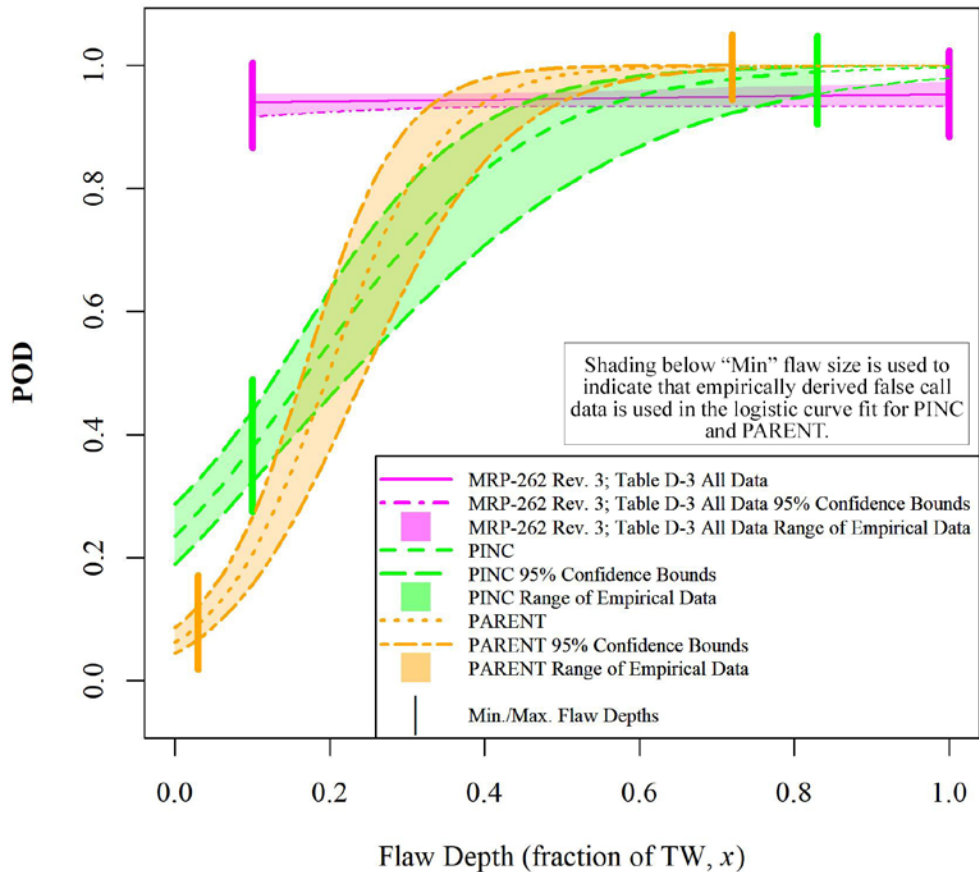


Figure 4.1. Plots of POD as a Function of Flaw Depth (fraction of TW, x) for Circumferentially Oriented Flaws in SBDMW Test Blocks in PINC, PARENT, and PDI Efforts (OD Access)

Table 4.1. Tabulation of POD at Discrete Flaw Depth Sizes (fraction of TW, x) for Circumferentially Oriented Flaws in SBDMW Test Blocks in PINC, PARENT, and PDI Efforts

Fraction of TW Depth, x	MRP-262 Rev. 3; Table D-3 All Data	PINC Aggregate	PARENT Aggregate
0	NA	0.23	0.06
0.1	0.94	0.38	0.21
0.2	0.94	0.55	0.51
0.3	0.94	0.71	0.80
0.4	0.94	0.83	0.94
0.7	0.95	0.97	1.0
1.0	0.95	1.0	1.0

Table 4.2. Summary of the “Beta” Parameters Defining the Logistic Functions and Uncertainties for POD Curves Generated in Figure 4.1 for Circumferentially Oriented Flaws in SBDMW Test Blocks for PINC, PARENT, and PDI Efforts

	MRP-262 Rev. 3; Table 6-8 All Data	PINC Aggregate	PARENT Aggregate
β_1	2.71	-1.18	-2.71
β_2	0.31	6.9	13.7
σ_{β_1}	0.21	0.14	0.18
σ_{β_2}	0.45	1.0	1.5
$\rho_{\beta_1\beta_2}$	-0.86	-0.49	-0.48
Min. Flaw Depth, x	0.10 ^(a)	0.10	0.03
Max. Flaw Depth, x	1.00 ^(a)	0.83	0.72

(a) Minimum and maximum flaw sizes indicated for PDI datasets are based on the flaw size distribution requirements in Supplement 10 of Appendix VIII of Section XI of the American Society of Mechanical Engineers Boiler & Pressure Vessel Code and may not reflect the actual minimum and maximum flaw sizes in the PDI datasets.

4.2 Probability of Detection for Axial Flaws in Small Bore Dissimilar Metal Weld Components

POD curves derived as a function of flaw depth for axially oriented flaws in SBDMW test blocks in PINC, PARENT, and PDI efforts are presented in Figure 4.2. A tabulation of POD values from these curves at discrete flaw depth sizes is provided in Table 4.3. The beta parameters defining the logistic functions of the POD curves in Figure 4.2, and their uncertainties, is provided in Table 4.4. These results are obtained for OD access to SBDMWs.

For the axial flaw results in Figure 4.2, the PDI-generated curve exhibits more curvature than for the circumferential flaw results and exhibits good agreement with PARENT data for flaw sizes larger than 0.35–0.40 TW. The PINC and PARENT curves exhibit greater variability with respect to each other in comparison to the circumferential flaw case. These studies incorporated a greater number of circumferential flaws than axial flaws and it is possible that the sample size contributes to this greater variation.

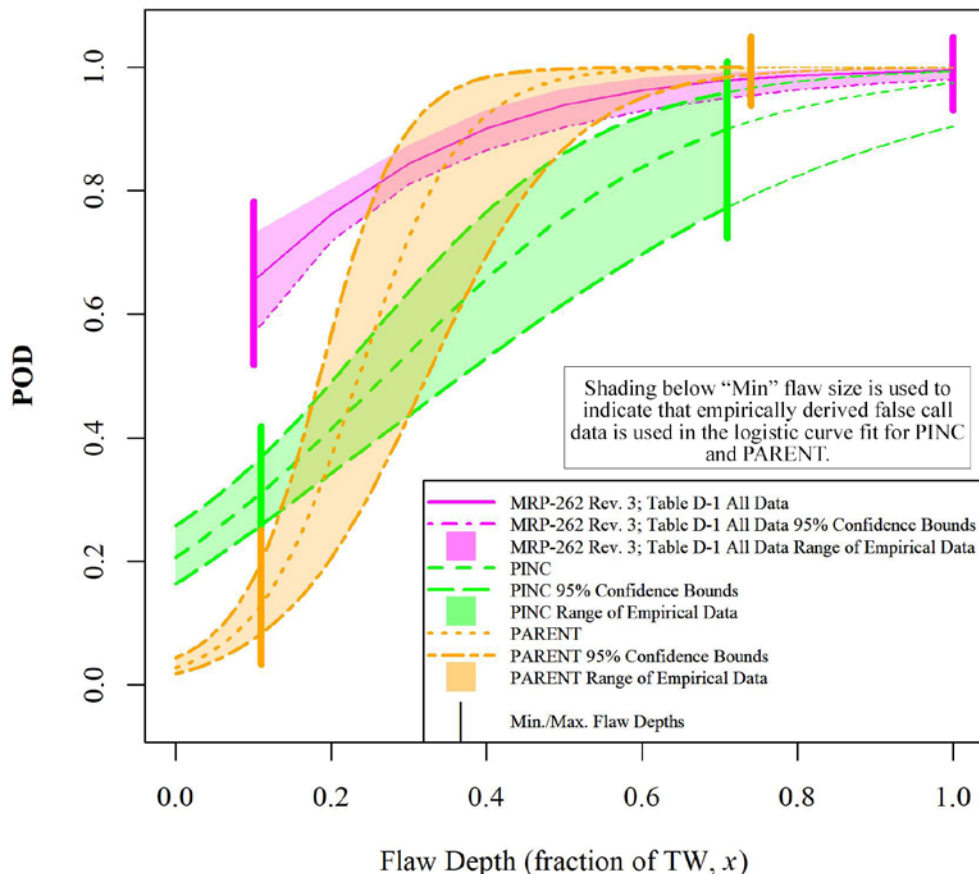


Figure 4.2. Plots of POD as a Function of Flaw Depth (fraction of TW, x) for Axially Oriented Flaws in SBDMW Test Blocks in PINC, PARENT, and PDI Efforts (OD Access)

Table 4.3. Tabulation of POD at Discrete Flaw Depth Sizes (fraction of TW, x) for Axially Oriented Flaws in SBDMW Test Blocks in PINC, PARENT, and PDI Efforts

Fraction of TW Depth, x	MRP-262 Rev. 3; Table D-1 All Data	PINC Aggregate	PARENT Aggregate
0	NA	0.21	0.03
0.1	0.66	0.30	0.11
0.2	0.76	0.41	0.37
0.3	0.84	0.54	0.73
0.4	0.90	0.66	0.92
0.7	0.98	0.90	1.0
1.0	1.0	0.97	1.0

Table 4.4. Summary of the “Beta” Parameters Defining the Logistic Functions and Uncertainties for POD Curves Generated in Figure 4.2 for Axially Oriented Flaws in SBDMW Test Blocks for PINC, PARENT, and PDI Efforts

	MRP-262 Rev. 3; Table 6-5 All Data	PINC Aggregate	PARENT Aggregate
β_1	0.12	-1.34	-3.56
β_2	5.24	4.99	15.1
σ_{β_1}	0.27	0.15	0.23
σ_{β_2}	1.02	0.77	2.3
$\rho_{\beta_1\beta_2}$	-0.91	-0.46	-0.43
Min. Flaw Depth, x	0.10 ^(a)	0.11	0.11
Max. Flaw Depth, x	1.00 ^(a)	0.71	0.74

(a) Minimum and maximum flaw sizes indicated for PDI datasets are based on the flaw size distribution requirements in Supplement 10 of Appendix VIII of Section XI of the American Society of Mechanical Engineers Boiler & Pressure Vessel Code and may not reflect the actual minimum and maximum flaw sizes in the PDI datasets.

4.3 Probability of Detection for Inner Diameter Access to Small Bore Dissimilar Metal Weld Components

POD curves derived as a function of flaw depth for circumferentially and axially oriented flaws in SBDMW test blocks in PINC are presented in Figures 4.3 and 4.4, respectively, for ID access. A tabulation of POD values from these curves at discrete flaw depth sizes is provided in Table 4.5. The beta parameters defining the logistic functions of the POD curves in Figures 4.3 and 4.4, and their uncertainties, is provided in Table 4.6.

The curves in Figures 4.3 and 4.4 are presented without comparison to PARENT or PDI analyses because no data was collected from comparable test blocks (wall thickness) by ID access (see Table 2.1).

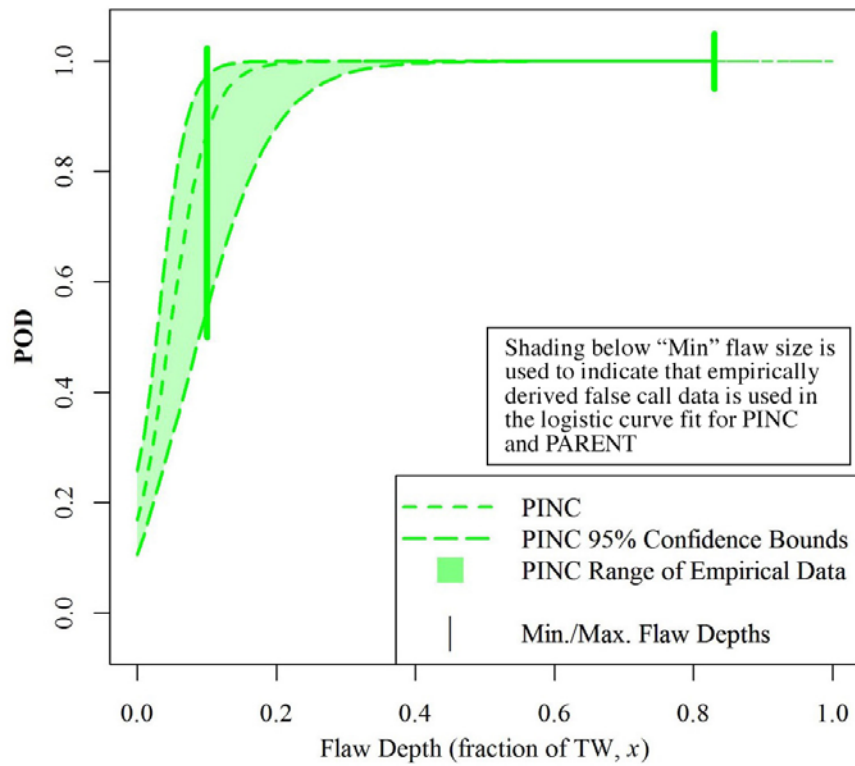


Figure 4.3. POD as a Function of Flaw Depth (fraction of TW, x) for Circumferentially Oriented Flaws in SBDMW Test Blocks in PINC (ID Access)

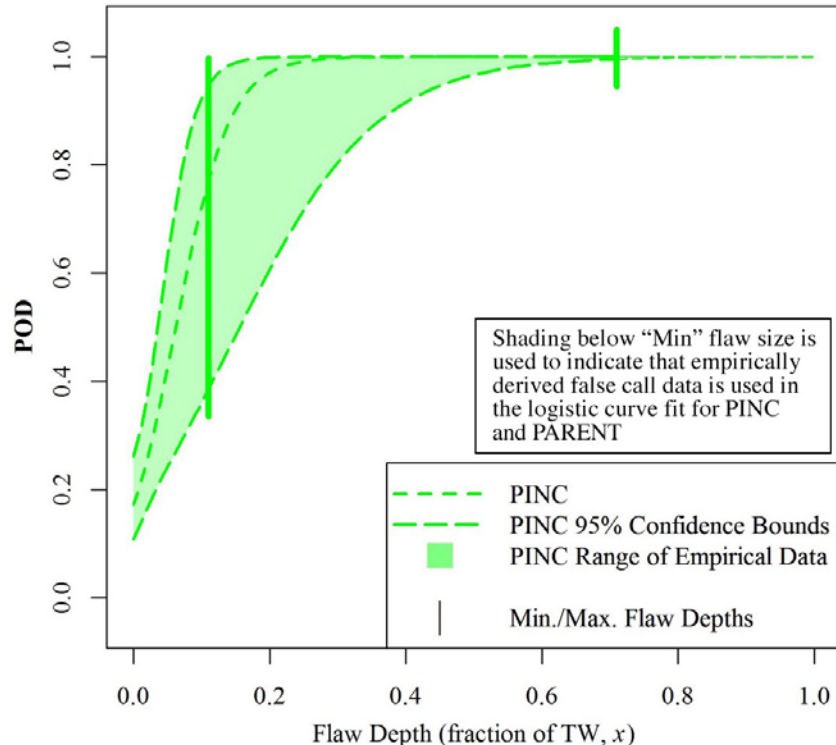


Figure 4.4. POD as a Function of Flaw Depth (fraction of TW, x) for Axially Oriented Flaws in SBDMW Test Blocks in PINC (ID Access)

Table 4.5. Tabulation of POD at Discrete Flaw Depth Sizes (fraction of TW, x) for POD Curves Generated in Figure 4.3 (circumferential flaws) and Figure 4.4 (axial flaws) for SBDMW Test Blocks and for ID Access for PINC

Fraction of TW Depth, x	Circumferential Flaws (Figure 4.3)	Axial Flaws (Figure 4.4)
0	0.17	0.17
0.1	0.87	0.72
0.2	1.0	0.97
0.3	1.0	1.0
0.4	1.0	1.0
0.7	1.0	1.0
1.0	1.0	1.0

Table 4.6. Summary of the “Beta” Parameters Defining the Logistic Functions and Uncertainties for POD Curves Generated in Figure 4.3 (circumferential flaws) and Figure 4.4 (axial flaws) for SBDMW Test Blocks and for ID Access for PINC

	Circumferential Flaws (Figure 4.3)	Axial Flaws (Figure 4.4)
β_1	-1.6	-1.57
β_2	35.1	25.4
σ_{β_1}	0.28	0.27
σ_{β_2}	8.9	8.0
$\rho_{\beta_1\beta_2}$	-0.23	-0.24
Min. Flaw Depth, x	0.10	0.11
Max. Flaw Depth, x	0.83	0.71

5.0 Probability of Detection for Large Bore Dissimilar Metal Weld Components

This section presents the results of POD analysis for LBDMW components in PARENT and PDI. For PDI, Category B1 (RPV nozzle) components are comparable to PARENT LBDMW test blocks based on the similarity in dimensions (see Table 2.1). Comparisons may only be made for the data acquired by ID access because that is the only data included for the analysis of PDI Category B1 components (see Table 2.1). Results obtained by OD access of LBDMW test blocks in PARENT are presented separately. Data is also obtained by OD access of PDI Category B2 (steam generator nozzle) components. However, the thickness of Category B2 components is significantly greater than the thickness of PARENT LBDMW test blocks. Thus, results of POD analysis for PDI Category B2 components are presented separately from the results of POD analysis of data obtained by the OD access of LBDMW components in PARENT. The results of POD analysis for PARENT LBDMW test blocks for ID access and PDI Category B1 components are presented as POD versus TW depth for circumferentially and axially oriented flaws in Sections 5.1 and 5.2, respectively. A similar presentation of results for PARENT LBDMW test blocks for OD access is provided in Section 5.3 and for PDI Category B2 components, a presentation of results is provided in Section 5.4.

5.1 Probability of Detection for Circumferential Flaws in Large Bore Dissimilar Metal Weld Components

POD curves derived as a function of flaw depth for circumferentially oriented flaws in LBDMW test blocks in PARENT and PDI efforts are presented in Figure 5.1 (ID access). A tabulation of POD values from these curves at discrete flaw depth sizes is provided in Table 5.1. The beta parameters defining the logistic functions of the POD curves in Figure 5.1, and their uncertainties, is provided in Table 5.2.

Figure 5.1 indicates good agreement between PDI and PARENT data for all flaw sizes greater than 0.1 TW. High performance is predicted by both curves, regardless, and the agreement exhibited between the two curves is likely caused by the saturation of the curves near $POD = 1$ (i.e., POD is nearly maxed-out in both PDI and PARENT studies and is unable to discriminate any actual differences in performance if they exist).

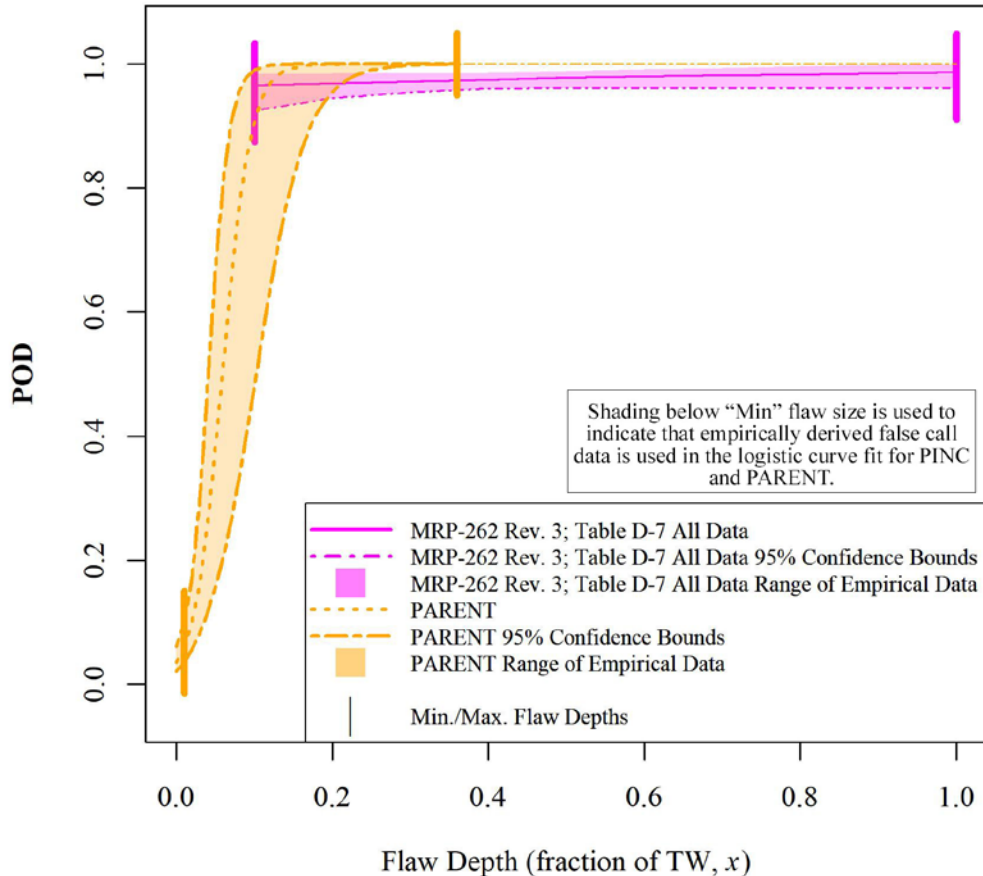


Figure 5.1. Plots of POD as a Function of Flaw Depth (fraction of TW, x) for Circumferentially Oriented Flaws in LBDMW Test Blocks in PARENT and PDI Efforts (ID Access)

Table 5.1. Tabulation of POD at Discrete Flaw Depth Sizes (fraction of TW, x) for Circumferentially Oriented Flaws in LBDMW Test Blocks in PARENT and PDI Efforts (ID Access)

Fraction of TW Depth, x	MRP-262 Rev. 3; Table D-7 All Data	PARENT ID Aggregate
0	NA	0.04
0.1	0.97	0.91
0.2	0.97	1.0
0.3	0.97	1.0
0.4	0.98	1.0
0.7	0.98	1.0
1.0	0.99	1.0

Table 5.2. Summary of the “Beta” Parameters Defining the Logistic Functions and Uncertainties for POD Curves Generated in Figure 5.1 for Circumferentially Oriented Flaws in LBDMW Test Blocks for PARENT and PDI Efforts (ID Access)

	MRP-262 Rev. 3; Table 6-14 All Data	PARENT ID Aggregate
β_1	3.24	-3.31
β_2	1.06	56
σ_{β_1}	0.55	0.29
σ_{β_2}	1.32	13
$\rho_{\beta_1\beta_2}$	-0.87	-0.33
Min. Flaw Depth, x	0.10 ^(a)	0.01
Max. Flaw Depth, x	1.00 ^(a)	0.36

(a) Minimum and maximum flaw sizes indicated for PDI datasets are based on the flaw size distribution requirements in Supplement 10 of Appendix VIII of Section XI of the American Society of Mechanical Engineers Boiler & Pressure Vessel Code and may not reflect the actual minimum and maximum flaw sizes in the PDI datasets.

5.2 Probability of Detection for Axial Flaws in Large Bore Dissimilar Metal Weld Components

POD curves derived as a function of flaw depth for axially oriented flaws in LBDMW test blocks in PARENT and PDI efforts are presented in Figure 5.2 (ID access). A tabulation of POD values from these curves at discrete flaw depth sizes is provided in Table 5.3. The beta parameters defining the logistic functions of the POD curves in Figure 5.2, and their uncertainties, is provided in Table 5.4.

In comparison to circumferential flaw results in Figure 5.1, the axial flaw results in Figure 5.2 also indicate relatively good agreement for PDI and PARENT data, although in this case, the “knee” in the PARENT curve is more gradual and located at approximately 0.3 TW. The PDI curve predicts slightly lower performance for the axial flaws in comparison to the circumferential flaws.

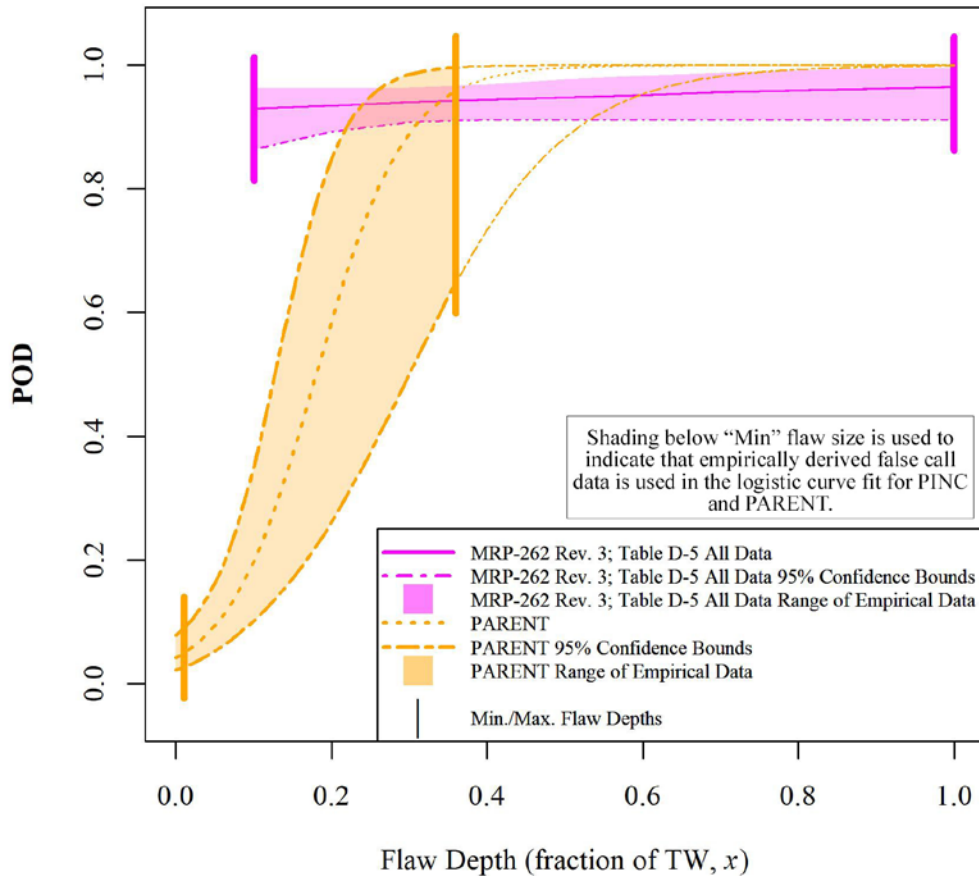


Figure 5.2. Plots of POD as a Function of Flaw Depth (fraction of TW, x) for Axially Oriented Flaws in LBDMW Test Blocks in PARENT and PDI Efforts (ID Access)

Table 5.3. Tabulation of POD at Discrete Flaw Depth Sizes (fraction of TW, x) for Axially Oriented Flaws in LBDMW Test Blocks in PARENT and PDI Efforts (ID Access)

Fraction of TW Depth, x	MRP-262 Rev. 3; Table D-5 All Data	PARENT ID Aggregate
0	NA	0.04
0.1	0.93	0.20
0.2	0.93	0.59
0.3	0.94	0.89
0.4	0.94	0.98
0.7	0.96	1.0
1.0	0.97	1.0

Table 5.4. Summary of the “Beta” Parameters Defining the Logistic Functions and Uncertainties for POD Curves Generated in Figure 5.2 for Axially Oriented Flaws in LBDMW Test Blocks for PARENT and PDI Efforts (ID Access)

	MRP-262 Rev. 3; Table 6-11 All Data	PARENT ID Aggregate
β_1	2.50	-3.14
β_2	0.82	17.4
σ_{β_1}	0.51	0.35
σ_{β_2}	1.40	3.9
$\rho_{\beta_1\beta_2}$	-0.87	-0.40
Min. Flaw Depth, x	0.10 ^(a)	0.01
Max. Flaw Depth, x	1.00 ^(a)	0.36

(a) Minimum and maximum flaw sizes indicated for PDI datasets are based on the flaw size distribution requirements in Supplement 10 of Appendix VIII of Section XI of the American Society of Mechanical Engineers Boiler & Pressure Vessel Code and may not reflect the actual minimum and maximum flaw sizes in the PDI datasets.

5.3 Probability of Detection for Outer Diameter Access to Large Bore Dissimilar Metal Weld Components

POD curves derived as a function of flaw depth for circumferentially and axially oriented flaws in LBDMW test blocks in PARENT are presented in Figure 5.3 and Figure 5.4, respectively (OD access). A tabulation of POD values from these curves at discrete flaw depth sizes is provided in Table 5.5. The beta parameters defining the logistic functions of the POD curves in Figure 5.3 and Figure 5.4, and their uncertainties, is provided in Table 5.6.

The curves in Figure 5.3 and Figure 5.4 are presented without comparison to PINC or PDI analyses because no data was collected from comparable test blocks (wall thickness) by OD access (see Table 2.1).

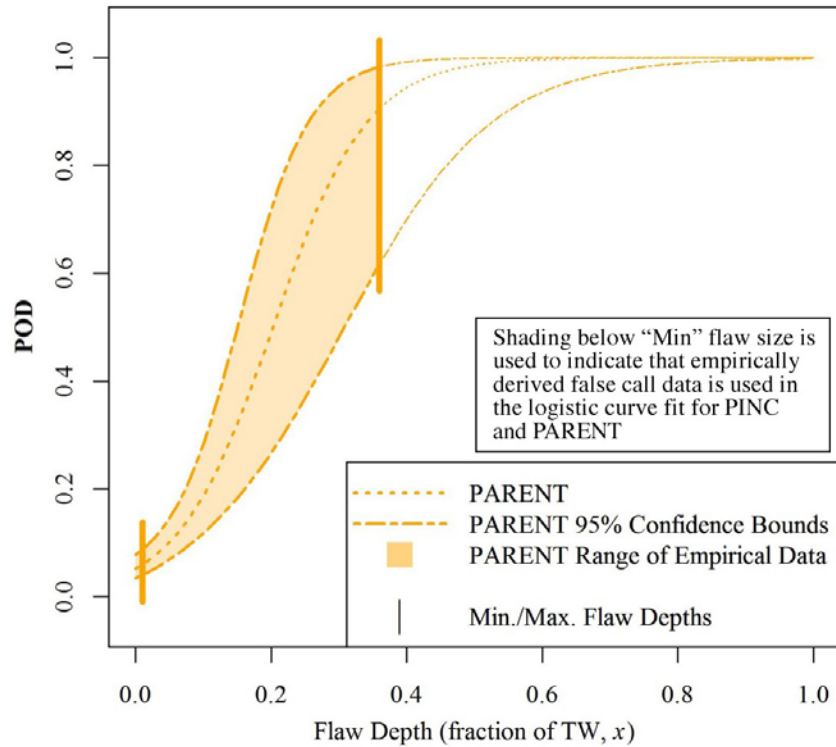


Figure 5.3. POD as a Function of Flaw Depth (fraction of TW, x) for Circumferentially Oriented Flaws in LBDMW Test Blocks in PARENT (OD Access)

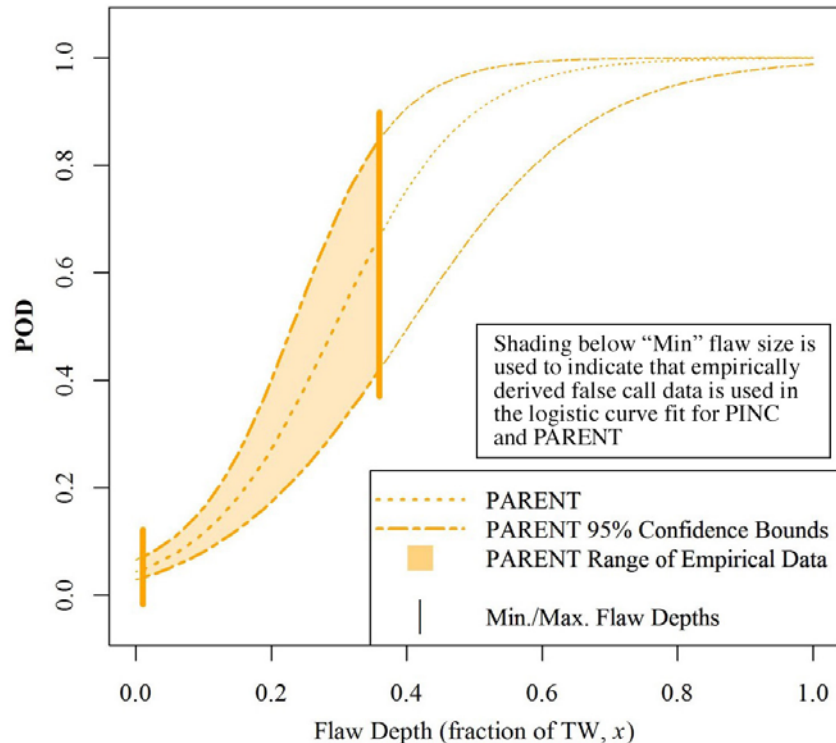


Figure 5.4. POD as a Function of Flaw Depth (fraction of TW, x) for Axially Oriented Flaws in LBDMW Test Blocks in PARENT (OD Access)

Table 5.5. Tabulation of POD at Discrete Flaw Depth Sizes (fraction of TW, x) for POD Curves Generated in Figure 5.3 (circumferential flaws) and Figure 5.4 (axial flaws)

fraction of TW depth, x	Circumferential Flaws (Figure 5.3)	Axial Flaws (Figure 5.4)
0	0.05	0.04
0.1	0.19	0.12
0.2	0.49	0.27
0.3	0.80	0.52
0.4	0.94	0.75
0.7	1.0	0.99
1.0	1.0	1.0

Table 5.6. Summary of the “Beta” Parameters Defining the Logistic Functions and Uncertainties for POD Curves Generated in Figure 5.3 (circumferential flaws) and Figure 5.4 (axial flaws)

	Circumferential Flaws (Figure 5.3)	Axial Flaws (Figure 5.4)
β_1	-2.91	-3.08
β_2	14.3	10.5
σ_{β_1}	0.22	0.22
σ_{β_2}	2.7	1.6
$\rho_{\beta_1\beta_2}$	-0.37	-0.46
Min. Flaw Depth, x	0.01	0.01
Max. Flaw Depth, x	0.36	0.36

5.4 Probability of Detection for Outer Diameter Access of PDI Category B2 (Steam Generator Nozzle) Components

This section presents the POD curve as a function of flaw depth obtained from PDI data for Category B2 (steam generator nozzle) components. This curve is generated from the parameter values reported in Table G-6 of MRP-262 Rev. 3 (EPRI 2017). This data is obtained by OD access of the test blocks. From Table 2.1, it is evident that Category B2 test blocks have a significantly larger thickness than Category B1 test blocks and test blocks categorized as LBDMWs in PARENT. The Category B2 data is presented independently for this reason. In MRP-262 Rev. 3, this data is provided in an appendix rather than the main body because of limitations with the data. It is stated that the data collected for the Category B2 analysis may not be applicable to field conditions because, although the mock-ups are relevant in thickness and diameter, they are unable to capture many relevant site-specific conditions for this component category. The POD curve based on parameters in Table G-6 of MRP-262 Rev. 3 is provided in Figure 5.5, and the values for the beta parameters are included in Table 5.7.

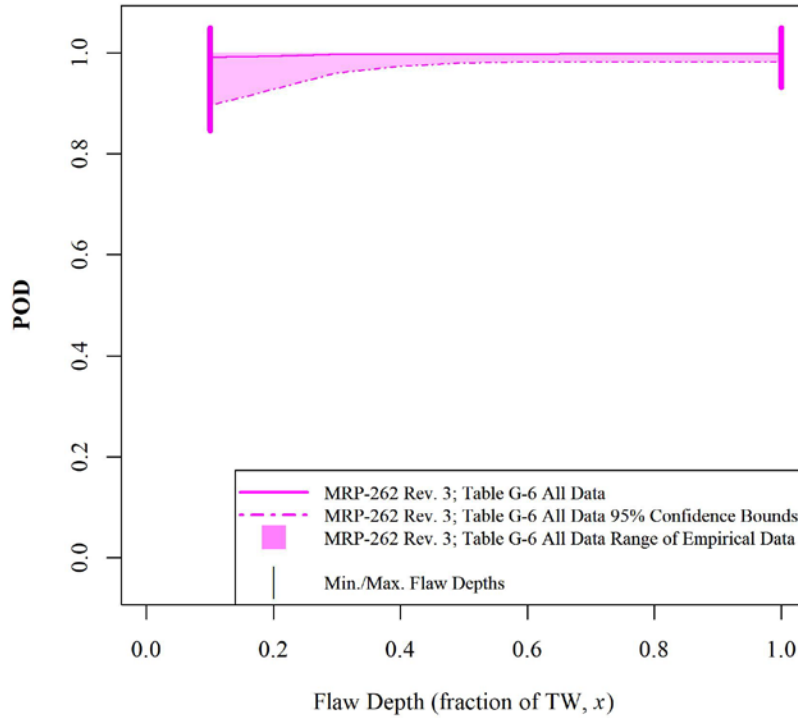


Figure 5.5. POD as a Function of Flaw Depth (fraction of TW, x) for Circumferentially Oriented Flaws in PDI Category B2 Components (EPRI 2017)

Table 5.7. Summary of the “Beta” Parameters Defining the Logistic Functions and Uncertainties for POD Curves Generated in Figure 5.5.

Circumferential Flaws (Figure 5.5)	
β_1	5.41
β_2	0.86
σ_{β_1}	3.64
σ_{β_2}	6.02
$\rho_{\beta_1\beta_2}$	-0.92
Min. Flaw Depth, x	0.10 ^(a)
Max. Flaw Depth, x	1.00 ^(a)

(a) Minimum and maximum flaw sizes indicated for PDI datasets are based on the flaw size distribution requirements in Supplement 10 of Appendix VIII of Section XI of the American Society of Mechanical Engineers Boiler & Pressure Vessel Code and may not reflect the actual minimum and maximum flaw sizes in the PDI datasets.

6.0 Discussion of Empirical Probability of Detection Analysis Results

This section provides discussion of the results presented in Sections 4.0 and 5.0 for SBDMW and LBDMW components, respectively. This discussion attempts to identify consistencies between the results of POD analyses based on data collected in PDI, PARENT, and PINC, and to present possible explanations for differences in the results. In addition, a discussion of the relevancy of these POD results to the field is also included followed by some recommendations.

6.1 Small Bore Dissimilar Metal Weld Probability of Detection Results

The analyses of POD on SBDMW components exhibit variability for the three studies (PDI, PINC, and PARENT). For the case of circumferential flaws (see Figure 4.1), results of analysis on PDI data exhibit a flat POD down to 0.1 TW flaw size. The POD curves for PINC and PARENT data exhibit more curvature with a “knee” transitioning from nearly saturated POD values for the large flaw size range to POD values that continue to decrease as the flaw size decreases to 0 TW. For flaw sizes greater than approximately 0.6 TW, all three curves predict a POD of 0.90 or greater. Thus, flaw size has a greater influence on POD in PINC and PARENT studies, at small flaw sizes, in comparison to results obtained from analysis of PDI data. The saturation of POD near $POD = 1.0$ for larger flaw sizes limits the ability of other factors to influence results as flaws become easier to detect, overall.

Similar observations can be made for POD analysis of axial flaws (see Figure 4.2). However, the discrepancy between PINC and PARENT curves appears larger than was observed for circumferential flaws. Also, the curve based on PDI data exhibits more curvature for axial flaws than for circumferential flaws, indicating a relatively greater influence of flaw size. In this case, the $POD = 0.90$ threshold is only crossed by all three curves for a relatively large flaw size (~0.8 TW) although the PARENT and PDI curves appear to both be across this threshold at 0.5 TW.

Results for data collected from the ID surface of SBDMW test blocks in PINC are provided for circumferential flaws and axial flaws in Figure 4.3 and Figure 4.4, respectively. In this case, there is no PARENT or PDI data for comparison. Essentially, these curves indicate that POD saturates at 1.0 for flaws approximately 0.2 TW or greater.

6.2 Large Bore Dissimilar Metal Weld Probability of Detection Results

Several cases of LBDMW POD results are presented in Section 5.0 and represent POD values generated from data collected from the ID surfaces of test blocks representing RPV nozzles, data collected from the OD surfaces of test blocks representing RPV nozzles, and data collected from the OD surfaces of test blocks representing steam generator nozzles. Results for the ID surfaces of RPV nozzle test blocks are presented in Figure 5.1 and Figure 5.2 for circumferential and axial flaws, respectively. Very good agreement is observed for PARENT and PDI data for circumferential flaws in Figure 5.1. For flaw sizes of 0.2 TW and above, both PARENT and PDI curves are relatively flat and exhibit POD values of 0.97 or greater.

The “knee” in the PARENT curve is located near 0.3 TW for axial flaws (see Figure 5.2). Above this flaw size, the PARENT and PDI curves are relatively flat and exhibit POD values of 0.89 or greater.

Results for data collected from the OD surface of LBDMW test blocks in PARENT are provided for circumferential flaws and axial flaws in Figure 5.3 and Figure 5.4, respectively. In this case, there is no PINC or PDI data for comparison. The transition in the plot of Figure 5.3 (circumferential flaws) appears sharper than the transition in Figure 5.4 (axial flaws). While it appears that near saturation of the POD curve occurs at 0.4 TW for circumferential flaws, this same feature occurs for axial flaws near 0.6 TW.

Finally, results obtained from the OD surface of Category B2 (steam generator nozzle) components in PDI are provided in Figure 5.5 for circumferential flaws. The curve appears saturated at POD = 1.0 for all flaw sizes of 0.1 TW and greater. However, caution is emphasized in MRP-262 Rev. 3 (EPRI 2017) with respect to limitations of the data supporting this the curve displayed in Figure 5.5. These limitations are noted in Section 5.4.

6.3 Contributions to Discrepancies in Results

The results of POD analyses performed on data collected from SBDMW test blocks exhibit significant variation between PINC, PARENT, and PDI (refer to Figure 4.1 and Figure 4.2). Several factors could contribute to this, particularly to differences between results based on PDI data with respect to PINC and PARENT data. Differences in the types of flaws used in the studies could contribute to the observed variation among studies. Further, the distribution of flaw sizes also varies among the datasets and this could also be a contributing factor to observed variations in POD estimations.

The format for the tests may also have an influence on results. PDI data is based on pass-fail screening examinations administered to candidates seeking qualification to perform examinations in the industry. EPRI administers the examinations and is custodian of the specimens. Candidates travel to EPRI facilities to perform their qualification examination. In PINC and PARENT, participants are expected to conduct a best-effort examination without expectation that their performance will impact their ability to practice in the industry. Further, the specimens were shipped to facilities convenient for participants to perform their examinations. As a result, results from PINC and PARENT may be more indicative of the performance that is possible under favorable conditions, while the results of PDI may be skewed by the practical objective of qualification to determine if performance exceeds the threshold for passing the PDI examination.

PINC and PARENT represent measurements of NDE performance at discrete points in time, 2007 to 2008 and 2012 to 2014, respectively, whereas data for PDI has been accumulated for nearly 20 years (EPRI 2017). Thus, the results in MRP-262 Rev. 3 represent an estimation of an average performance over that time frame. Assuming performance has been improving, this would suggest that PINC and PARENT should estimate better levels of performance than analysis of PDI data and that PARENT should estimate better performance than PINC.

The techniques and procedures applied in each effort vary and likely influenced the observed results. According to MRP-262 Rev. 3, the reported POD results are based on the analysis of ultrasonic inspection data, and more specific information about the types of ultrasonic testing techniques and procedures is not provided. In the PINC and PARENT efforts, SBDMW test blocks were examined from the OD surface using UT, PAUT, a combination of UT and PAUT, and a combination of UT and TOFD technique. Varying distributions of the numbers of specific techniques applied in each effort is likely to contribute to variation in the observed results.

Finally, differences in the way data is analyzed is also expected to have an influence on the generated POD curves for each data set. Although each effort fit data by logistic function regression, treatment of the condition of POD at zero flaw size varied among the studies. For PDI data, false call rate data was not

used in the fitting of logistic curves. In PINC and PARENT, the logistic function is fit over the entire flaw size range down to 0 TW using the value of FCP that is calculated from the empirically observed false call rate. However, different values of blank grading unit length, L_{gu} , [refer to Eqs. (4) and (5) in Section 2.3] were assumed in the analysis of PINC and PARENT data. This would lead to inconsistent calculations of FCP in Eq. (5) for a given false call rate [Eq. (4)]. The entire logistic model can be affected because the calculated FCP is a data point used for fitting the logistic model by MLE.

6.4 Relevance of Results to the Field

There are many aspects of a field examination that are impractical to replicate during PDI qualification exams or laboratory studies to assess NDE performance such as PINC and PARENT. The limitations of laboratory-based studies to replicate actual field conditions is well recognized and not limited to the nuclear power industry. Examples of field conditions that may be difficult or impossible to replicate in a laboratory study include stresses due to organizational pressures (e.g., influence of deadlines, revenue goals, etc.) or the environment (e.g., uncomfortable temperatures, anxiety over radiation exposure). In this context, it is expected that laboratory studies provide a favorable setting for performing an inspection compared to the field, which could result in a non-conservative estimation of POD for field applications.

Summaries of PWSCC events within the industry are provided in Appendices A and B of NUREG/CR-7187 (Sullivan and Anderson 2014). Leakages due to PWSCC have been reported on multiple occasions in butt welds joining vessel nozzles to reactor coolant piping. Although leakage from a circumferential flaw was reported in 1993 (Palisades), leakage events reported from PWSCC since then were associated with axial flaws (V.C. Summer – 2000, Tsuruga – 2003, Davis-Besse – 2008, North Anna – 2012). These events occurred in components that spanned both SBDMW and LBDMW dimensions. A summary of these events is provided in Table 6.1. These events confirm that flaws are sometimes missed by examinations in the field, but the size of the flaws at the time they were missed by examination is difficult to estimate. One exception is the 2012 event at North Anna that was observed after removal of material from a steam generator nozzle joint in preparation for a weld overlay. In this case, manual non-encoded UT examinations performed prior to the removal of the material missed several flaws, at least one of which was estimated to be 0.8 TW prior to the machining. The manual non-encoded UT procedure had been qualified with on site-specific mock-ups because of geometric conditions that were specific to the site. Note that no POD model is derived for axial flaws in Category B2 components in MRP-262 Rev. 3 (EPRI 2017), in part, because the variation in geometric conditions make it difficult to derive generically applicable results.

Overall, this field data is insufficient to rule out the possible relevancy of the POD models presented in this report. It is possible that the flaws associated with the events in Table 6.1 were sufficiently small at the time they were last examined that a reasonable probability of missing the flaw based on POD models presented in this report is expected. Also, given the time elapsed between some of these events and time data was collected in PARENT (2012–2014), it is also possible that performance has improved since the time at which many of these events occurred.

The scenarios for which PDI predicts lower POD at larger flaw sizes in comparison to PARENT and PINC data are not strongly represented in these field events. These scenarios include the SBDMW examinations by OD access for circumferential flaws and the LBDMW (Category B1) examination scenarios by ID access. ID access examinations are not represented in this sample of field events. Further, the only circumferential flaw event occurred at Palisades in 1993.

Table 6.1. Summary of Leakage Events from Appendix A and B of NUREG/CR-7187 (Sullivan and Anderson 2014)

Site	Year	Component	Category	Flaw Orientation
North Anna	2012	Reactor coolant loop hot-leg-to-steam generator nozzle weld	LBDMW (Category B2) – OD	Axial
V.C. Summer	2000	RPV nozzle-to-pipe weld	LBDMW (Category B1) – OD	Axial
Davis-Besse	2008	Decay heat removal to reactor coolant system nozzle weld	SBDMW – OD	Axial
Tsuruga	2003	Pressurizer relief and safety nozzle-to-safe-end welds	SBDMW – OD	Axial
Palisades	1993	Heat-affected zone of the pilot-operated relief valve Alloy 600 safe end	SBDMW – OD	Circumferential

6.5 Recommendations

A significant function of this report is to concisely summarize POD models for DMW components that have been generated from empirical data. A summary of the beta parameters, their standard deviations, and their covariances for POD models from Sections 4.0 and 5.0 is provided in Table 6.2, for convenience. Even though there are several potential factors leading to variation in PINC, PARENT, and PDI results, it is evident that there are cases in which the relevance of these factors is diminished by saturation of the curves at or near $POD = 1.0$. This is most strongly apparent in Figure 5.1 for the ID surface examination of LBDMW test blocks. It is also generally evident that variation diminishes as curves begin to saturate for large flaw sizes. For both SBDMWs and LBDMWs, it may suffice to use the POD estimates obtained from PDI for large flaw sizes, as they result in more conservative estimates in the large flaw size range. The one exception being for axial flaws in SBDMWs. In this case “large” flaw size is not precisely defined but is simply used to refer to the flaw size range in which all results indicated a POD of approximately 0.90 or greater.

For “small” flaw sizes, conservative POD estimates are generally provided by the PINC and PARENT results; however, use of engineering judgement for a specific application is always recommended. A study of the sensitivity of xLPR output to uncertainty in POD data was performed by Heasler et al. (2011). A conclusion of this study was that knowledge of POD for large flaws is more important than for small flaws. This is because a small flaw that is missed may be more likely to undergo additional examinations before it can grow large enough to cause rupture. However, like “large” flaw size, “small” flaw size is not precisely defined. Analyses to help determine (and quantitatively define) the flaw sizes for which accurate knowledge of POD is most important for the cases considered in this report would be beneficial to providing an improved understanding of the significance of the observed variability in POD results for these efforts.

Treatment of the POD value at 0 TW has a significant influence on POD values at the smaller flaw sizes, which is the flaw range for which most variation was observed between the results of PDI, PINC, and PARENT efforts. Future efforts could benefit from guidance (e.g., a consensus standard) on performing POD analyses on empirical NDE data. These experiences show that even after all data is collected, there are many aspects of the data analysis process that allow results to be subject to the judgement of the individual analyzer. Development of guidance could improve the consistency in which judgements are made in the analysis process.

Finally, a brief comparison of the POD models in this report to available field data is unable to yield strong conclusions regarding the representativeness of the models for field application or make a judgement about which models may provide a more accurate representation of field POD. A more extensive and systematic review of field events may yield stronger evidence regarding the accuracy of models with respect to field POD.

Table 6.2. Summary of POD Model “Beta” Parameters for the Models Summarized in Sections 4.0 and 5.0

Category	Flaw Orientation	Data Source	β_1	β_2	σ_{β_1}	σ_{β_2}	$\rho_{\beta_1\beta_2}$	Min. Flaw Depth, x	Max. Flaw Depth, x	
SBDMW (OD Access)	Circumferential	PDI – Category A (MRP-262 Rev. 3; Table 6-8)	2.71	0.31	0.21	0.45	-0.86	0.10 ^(a)	1.00 ^(a)	
		PINC		-1.18	6.9	0.14	1.0	-0.49	0.10	0.83
		PARENT		-2.71	13.7	0.18	1.5	-0.48	0.03	0.72
SBDMW (OD Access)	Axial	PDI – Category A (MRP-262 Rev. 3; Table 6-5)	0.12	5.24	0.27	1.02	-0.91	0.10 ^(a)	1.00 ^(a)	
		PINC		-1.34	4.99	0.15	0.77	-0.46	0.11	0.71
		PARENT		-3.56	15.1	0.23	2.3	-0.43	0.11	0.74
SBDMW (ID Access)	Circumferential	PINC	-1.6	35.1	0.28	8.9	-0.23	0.10	0.83	
SBDMW (ID Access)	Axial	PINC	-1.57	25.4	0.27	8.0	-0.24	0.11	0.71	
LBDMW (ID Access)	Circumferential	PDI – Category B1 (MRP-262 Rev. 3; Table 6-14)	3.24	1.06	0.55	1.32	-0.87	0.10 ^(a)	1.00 ^(a)	
		PARENT		-3.31	56	0.29	13	-0.33	0.01	0.36
LBDMW (ID Access)	Axial	PDI – Category B1 (MRP-262 Rev. 3; Table 6-11)	2.50	0.82	0.51	1.40	-0.87	0.10 ^(a)	1.00 ^(a)	
		PARENT		-3.14	17.4	0.35	3.9	-0.40	0.01	0.36
LBDMW (OD Access)	Circumferential	PARENT	-2.91	14.3	0.22	2.7	-0.37	0.01	0.36	
LBDMW (OD Access)	Axial	PARENT	-3.08	10.5	0.22	1.6	-0.46	0.01	0.36	
LBDMW (OD Access)	Circumferential	PDI – Category B2 (MRP-262 Rev. 3; Table G-4)	5.41	0.86	3.64	6.02	-0.92	0.10 ^(a)	1.00 ^(a)	

(a) Minimum and maximum flaw sizes indicated for PDI datasets are based on the flaw size distribution requirements in Supplement 10 of Appendix VIII of Section XI of the American Society of Mechanical Engineers Boiler & Pressure Vessel Code and may not reflect the actual minimum and maximum flaw sizes in the PDI datasets.

7.0 Summary and Conclusions

The accuracy of the ISI module in xLPR is dependent on the quality of the estimates of detection and sizing performance that are input to the module. In this report, a comparison of the POD estimates obtained from three efforts for DMW components (industry PDI, PINC, and PARENT) is performed. A summary of empirically derived POD models considered in this report is provided in Table 6.2. Comparisons of POD results are provided for both axial and circumferential flaws in SBDMW and LBDMW components with consideration also given to surface access (ID or OD). In general, significant variability between results is observed, especially for smaller flaw sizes. The PDI results provide the most conservative POD estimates for larger flaw sizes except for axial flaws in SBDMW components. Conversely, PINC or PARENT results provide more conservative results for smaller flaw sizes. The definitions of “small” and “large” flaw sizes are not precise in this context but are generally used to distinguish the flaw size range for which all results exhibit approximately $POD = 0.90$ or greater.

Overall, the following general observations can be made from the summarized POD models for PINC, PARENT, and industry PDI data:

- Significant variability exists between the POD models obtained from analysis of data from PINC, PARENT, and industry PDI data.
- Variability in POD models obtained from each data set is greater for “small” flaw size regimes than “large” flaw size regimes.
- Some of the observed variability in POD models can be attributed to inconsistencies in the way data from each study is analyzed.
- A preliminary comparison of the POD models with some reported industry events was unable to yield firm conclusions regarding how well models represent actual field POD.

Based on the observations above, the following suggestions for future work are provided:

- Perform sensitivity analyses to better understand the importance of the observed variability in POD models.
- Develop standard guidance for analyzing inspection data to estimate POD from sources such as PINC, PARENT, and PDI.
- Perform a systematic review of field events, and then compare field events with the POD models obtained from PINC, PARENT, and PDI data.

8.0 References

Ammirato F. 2009. *Development of Probability of Detection Curves for Ultrasonic Inspection of Dissimilar Metal Welds to Support Leak-Before-Break Assessment*. EPRI Report 1019088 (MRP-262). Palo Alto, California: Electric Power Research Institute.

Berens AP. 1989. "NDE Reliability Data Analysis." In *ASM Handbook, Volume 17: Nondestructive and Quality Control*, pp. 689-701. Materials Park, Ohio: ASM International.

Cumblidge SE, SR Doctor, PG Heasler and TT Taylor. 2010. *Results of the Program for the Inspection of Nickel Alloy Components*. NUREG/CR-7019; PNNL-18713, Rev. 1. Washington, DC: U.S. Nuclear Regulatory Commission.

EPRI. 2017. *Development of Probability of Detection Curves for Ultrasonic Inspection of Dissimilar Metal Welds: Typical PWR Leak-Before-Break Line Locations*. EPRI Report 3002010988 (MRP-262, Revision 3). Palo Alto, California: Electric Power Research Institute.

Forsyth DS and A Fahr. 1998. "An Evaluation of Probability of Detection Statistics." In *Research and Technology Organization Applied Vehicle Technology Workshop on Airframe Inspection Reliability under Field/Depot Conditions (RTO MP-10)*, pp. 10-1 to 10-5. May 13-14, 1998, Brussels, Belgium. RTO/NATO, Cedex, France.

Heasler PG, SE Sanborn, SR Doctor and MT Anderson. 2011. "The Treatment of ISI Uncertainty in Extremely Low Probability of Rupture." In *Proceedings of the ASME 2011 Pressure Vessels & Piping Division Conference*, pp. 1061-1067. July 17-21, 2011, Baltimore, Maryland. DOI 10.1115/PVP2011-57975. ASME, New York.

Meyer RM and PG Heasler. 2017. *Results of Blind Testing for the Program to Assess the Reliability of Emerging Nondestructive Techniques*. NUREG/CR-7235, PNNL-24196. Washington, D.C.: U.S. Nuclear Regulatory Commission. ADAMS Accession No. ML17159A466.

NRC. 2007. *Standard Review Plan for the Review of Safety Analysis Reports for Nuclear Power Plants: LWR Edition, Section 3.6.3, Leak-Before-Break Evaluation Procedures, Revision 1*. NUREG-0800, Rev. 1. Washington, D.C.: U.S. Nuclear Regulatory Commission.

Rudland D, C Harrington and R Dingreville. 2015. "Development of the Extremely Low Probability of Rupture (xLPR) Version 2.0 Code." In *ASME 2015 Pressure Vessels and Piping Conference*, p. V06BT06A050. July 19–23, 2015, Boston, Massachusetts. DOI 10.1115/PVP2015-45134. ASME, New York.

Sullivan EJ and MT Anderson. 2014. *Managing PWSMC in Butt Welds by Mitigation and Inspection*. NUREG/CR-7187, PNNL-23659. Washington, D.C.: U.S. Nuclear Regulatory Commission.



**Pacific
Northwest**
NATIONAL LABORATORY

www.pnnl.gov

902 Battelle Boulevard
P.O. Box 999
Richland, WA 99352
1-888-375-PNNL (7665)



Prepared for the U.S. Nuclear Regulatory Commission
under a Related Services Agreement with the U.S. Department of Energy
CONTRACT DE-AC05-76RL01830

U.S. DEPARTMENT OF
ENERGY